γ-ray Compton profile of polycrystalline lithium

S. Wachtel,* J. Felsteiner, S. Kahane, and R. Opher†
Department of Physics, Technion-Israel Institute of Technology, Haifa, Israel
(Received 21 May 1974)

The Compton profile of polycrystalline lithium has been measured using a ^{241}Am source of 59.54-keV γ rays. In this work the high-momentum region up to 3 a.u. was investigated and a non-negligible tail was observed in the Compton profile. Previously reported x-ray measurements did not extend into the momentum region beyond 1.6 a.u. The contribution of the two core electrons was substracted from the data using free-atom wave functions. The resultant conduction-electron profile was first compared with calculations in the cell approximation in which the electron-ion interactions are represented by a model using s-like wave functions. In particular such functions were computed in the renormalized free-atom model, previously employed by Berggren for calculation of the Compton profile of vanadium. Next, electron-electron interactions were taken into account in the former calculation by introducing occupation numbers obtained for an homogeneous interacting electron gas using a method due to Lam. The results indicate that the existence of the high-momentum tail in the profile is mainly due to the electron-ion interactions. This is in accord with recent work of Eisenberger *et al.*, but in contradiction with Phillips and Weiss who attributed this tail to electron-electron correlations.

I. INTRODUCTION

During the last few years there has been an increasing experimental and theoretical interest in the Compton profile of lithium.[1-7] The small number of electrons per atom together with the large relative number of conduction electrons, 1:3, makes it a convenient material for Compton-profile measurements. Furthermore, the correlation effects between the conduction electrons and the electron-ion interactions are not well known and it is of great interest to investigate their relative contributions to the Compton profile and to the electron-momentum density.

Compton-profile measurements on lithium have been reported by Cooper *et al.*,[1,2] Phillips and Weiss,[3,4] and Eisenberger *et al.*[5] All these measurements employed low-energy x rays, a fact that limited them to only small momenta ($q \lesssim 1.6$ a.u.). It is expected that the electron-electron correlations and the electron-ion interactions might give some contribution in the high-momentum region. In the present work we performed a new measurement of the Compton profile of polycrystalline lithium using 59.54-keV ^{241}Am γ rays, which extended to momenta up to 3 a.u.

A number of theoretical investigations have been reported which may be divided into two kinds. In the first kind, wave functions for the conduction electrons are calculated in the one-electron approximation and the momentum density and Compton profile are deduced. This approach has been used by Donovan and March[6] and later by Cooper *et al.*[1] and Borland and Cooper,[2] and was not successful in fitting theory with experiment. In the second kind of theories many-body effects such as electron-electron correlations are taken into account using, for instance, electron-gas calculations.[7,8] Recently, two different approaches have been made in order to derive the momentum density and Compton profile for an interacting electron gas submerged in a lattice of static ions. The Hamiltonian of the electronic system may be written as $H = T + V + U$, where T represents the kinetic energy, V the electron-ion interaction, and U the electron-electron interaction. Eisenberger *et al.*[5] treated V as the perturbation and $T + U$ as the unperturbed part, while Lundqvist and Lyden[9] chose to start with $T + V$ as the unperturbed part. The last approach seems to be a more convenient one if the momentum distribution has been calculated in a first step from some one-electron model.

For comparison with the previous Compton-profile data, all the above calculations were reported only up to about 1.6 a.u. Tan[10] calculated the Compton profile up to 2 a.u. for a lithium single crystal using Callaway-Kohn-Silverman wave functions. In order to give an interpretation of the present measurements, it is necessary to calculate the Compton profile up to 3 a.u. For this purpose we followed the approach of Lundqvist and Lyden.[9] The momentum density and Compton profile were first computed in the cell approximation using isotropic s-like functions. Following the calculation of Berggren on polycrystalline vanadium[11] we used the renormalized-free-atom model (RFA), which makes a compromise between a complete band-structure calculation and a free-atom description. Electron-electron interactions were then incorporated in these calculations by employing mean occupation numbers calculated for an homogeneous electron gas using an approach due to Lam.[8] Finally, the experimental and theoretical results were compared in order to assess

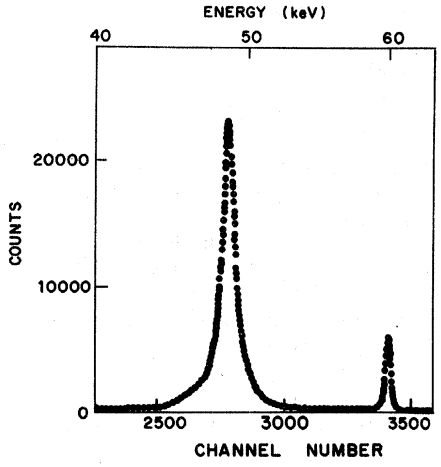

FIG. 1. Total spectrum obtained after a 100-h run. The error bars are smaller than the size of the data points.

the relative importance of the various interactions in lithium.

II. EXPERIMENTAL PROCEDURE

A Compton-profile measurement was made at room temperature using 59.54-keV γ rays of ^{241}Am, scattered from the sample through an angle of $(161 \pm 3)°$. The apparatus is similar to that previously described.[12] The distance between the source and the target was 17 cm. The intensity of the source was 300 mCi. The Compton peak for the above experimental angle is at 48.55 keV. The target was a thin polycrystalline lithium sample. Its thickness (0.5 cm) is much smaller than the mean free path in lithium for 60-keV photons (~12.5 cm), so that absorption and multiple-scattering effects are not expected to be appreciable,[13] which is an advantage on previous x-ray measurements.[4,5] On the other hand, the net counting rate from the sample is low and the relative contribution of the scattering from the air behind the sample will be very large. We took care of this by placing behind the target a lead sheet which has a high photoelectric to Compton cross-section ratio, so that the counting rate due to the background was significantly reduced. The measured background (with no sample) is in this case a very good approximation to the true background (with sample), since a thin lithium sample will have a negligible effect on scattering from the lead backing.

The resolution function of the detector and the electronic system was found to be mainly a Gaussian with a full width at half-maximum (FWHM) of 415 eV at 60 keV. In addition, there is a smearing of the profile due to the geometrical arrangement which could be approximated by a Gaussian. The width of the total resolution function of the system obtained by convolution of the two Gaussians turned out to be 425 eV.

The gain of the detection system was arranged so that the data could be taken at intervals of 17.5 eV/channel. Figure 1 shows the raw experimental data obtained after a period of 100 h. Approximately 23 000 counts/channel were accumulated at the center of the profile. Background measurement was made and subtracted from the total spectrum after proper normalization. It contributed about 4000 counts/channel at the center of the profile. The net Compton spectrum after removal of the background is shown in Fig. 2. We show in Fig. 3 the raw data above $q = 1$ a.u. on an expanded scale, together with the lead-backing contribution and the contribution of the core electrons in lithium.

The aim of the data reduction was to substract all the energy-dependent contributions that might influence the shape of the spectrum and do not originate from the specific Compton scattering from lithium. The detector efficiency (that is, the fraction of photons at a given energy which strike the detector and contribute to a pulse in the multichannel analyzer) is approximately unity at energies smaller than 60 keV and its variation within the considered energy range could be neglected.

An evaluation of the absorption in the air between the sample and the detector and in the beryllium window of the detector showed that the energy dependence is negligible in our experimental conditions. (The variation of the correction factor as a function of energy as defined by Eisenberger and Reed[14] was smaller than 0.12% over the whole region of interest for the air absorption

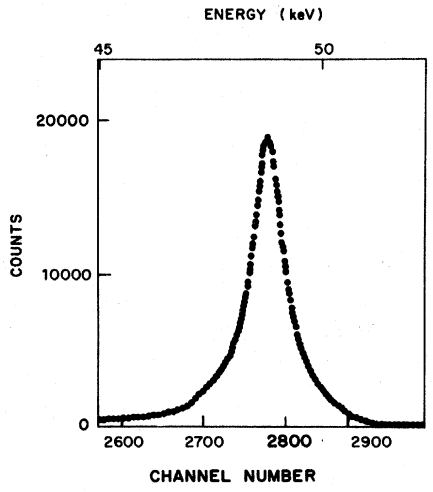

FIG. 2. Compton profile after background substraction. The error bars are smaller than the size of the data points.

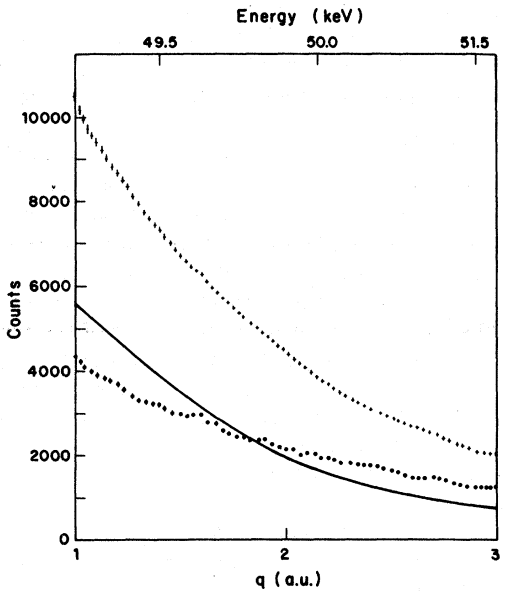

FIG. 3. Raw data above $q = 1.0$ a.u. on an expanded scale, with lead backing and core contributions: (a) (++++) raw data; (b) (····) lead backing; (c) (——) lithium core.

and about 0.04% for the absorption due to the beryllium window.) Furthermore, an evaluation of the correction factor for the absorption in the sample showed that for 0.5-cm thickness the variation within our whole energy range was 0.08% and could be neglected to a good approximation.

The deconvolution of the profile which accounts for the above calculated finite resolution was made using a procedure due to Lloyd.[15] In addition to the Gaussian shape assumed above, a low-intensity tail on the low-energy side of the resolution function was observed (with a peak-to-tail ratio of 130/1) and it could be approximated as a straight line. The contribution of this tail was substracted successively from all the channels. We obtained an intensity which is proportional to the Compton differential cross section $d^2\sigma/d\omega d\Omega$ and the final Compton profile for all the electrons in lithium can be written[12]

$$J(q) \propto \frac{\omega_0 |\Delta k|}{\omega} \frac{d^2\sigma}{d\omega\, d\Omega} , \tag{1}$$

where ω_0 and ω are the initial and final photon energies and Δk is the momentum transfer. q is the electron-momentum component along the direction of Δk and is given in the case of lithium by[12]

$$q = \tfrac{1}{2}|\Delta k| + (\Delta\omega/|\Delta k|)m - (\Delta\omega)^2/2|\Delta k| , \tag{2}$$

with $\Delta\omega = \omega - \omega_0$. The Compton profile for all the electrons is normalized to

$$\int_0^\infty J(q)\, dq = 1 \text{ per electron.} \tag{3}$$

The integration was performed on the high-energy side of the profile because the energy-dependent corrections, which resulted in the removal of the asymmetry of the spectrum, led to larger errors in the low-energy side of the profile. The $q = 0$ point was first calculated by Eq. (2) using the scattering angle previously measured. This was compared with the $q = 0$ point obtained from the condition[14]

$$\int_0^{1\,\text{a.u.}} J(q)\, dq = \int_{-1\,\text{a.u.}}^{0} J(q)\, dq . \tag{4}$$

It was found that these two points differed by less than 0.03 a.u. of q or 18.5 eV of photon energy. The spectrum obtained is presented in Fig. 4. A correction to the normalization of this profile using the Waller–Hartree theory[16] was calculated and found to be negligible in the present large energy transfer conditions.

The contribution of the core electrons to the spectrum was calculated in the impulse approximation using free atom functions,[17] therefore yielding the Compton profile of the conduction electrons which was normalized to

$$\int_0^{3\,\text{a.u.}} J(q)\, dq = 1 \tag{5}$$

The final normalized curve is shown in Figs. 7 and 8 and the numerical results are presented in Table I. The normalization was performed using a much finer table with a distance of 0.05 a.u. between consecutive points.

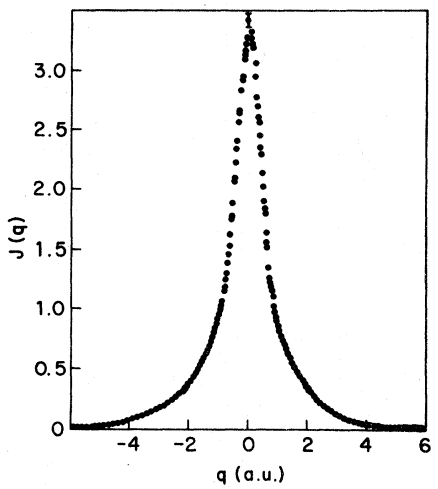

FIG. 4. Compton profile for three electrons in Li after all corrections have been made.

III. THEORY

A. Compton-profile calculation in cell approximation

The Compton profile for a polycrystalline sample can be defined as[12]

$$J(q) = 2\pi \int_q^\infty \langle \rho(\vec{p}) \rangle p \, dp \ , \tag{6}$$

where $\langle \rho(\vec{p}) \rangle$ is the spherical average of the electron-momentum density $\rho(\vec{p})$. From the knowledge of the one-electron wave function $\varphi_{\vec{k}}(\vec{r})$ for the electron in a solid lattice, the momentum transform $\varphi_{\vec{k}}(\vec{p})$ may be extracted and[11]

$$\rho(\vec{p}) = \sum_{\vec{k}} |\varphi_{\vec{k}}(\vec{p})|^2 \ , \tag{7}$$

where $\vec{k}$ is the wave vector of the electron.

In the cell approximation,[18] the solid is built up from units or cells, each of which is assumed to contain one atom (ion) and, in the alkali case, one conduction electron is moving essentially in the spherical potential of the ion. The cell as a whole is therefore neutral and the connection between neighboring cells is made by the use of the Wigner-Seitz condition:[18]

$$\left. \frac{\partial \varphi_{\vec{k}=0}}{\partial r} \right|_{r=r_s} = 0 \ , \tag{8}$$

where r_s is the radius of a sphere having a volume equal to that of the Wigner-Seitz cell.

We use here a procedure due to Berggren[11] that proved to be quite satisfactory in the case of vanadium. (Both vanadium and lithium have a bcc structure.) The Bloch function in the cell approximation is assumed to be

$$\varphi_{\vec{k}}(\vec{r}) = e^{i\vec{k}\cdot\vec{r}} \varphi_{\vec{k}=0}(\vec{r}) \ . \tag{9}$$

More precisely, $\varphi_{\vec{k}}(\vec{r})$ is usually expanded in a power series in k.[19] Nevertheless, calculations by Donovan and March[6] for lithium show that the higher orders of k are negligible and do not influence the shape of the Compton profile, thus justifying Eq. (9).

The momentum transform of the Bloch function is given by[11]

$$\varphi_{\vec{k}}(\vec{p}) = N \delta_{\vec{p},\vec{k}+\vec{G}_i} \varphi^c_{\vec{k}}(\vec{p}) \ , \tag{10}$$

where

$$\varphi^c_{\vec{k}}(\vec{p}) = (2\pi)^{-3/2} \int_{\Omega_0} d\vec{r} \, e^{-i\vec{p}\cdot\vec{r}} \varphi_{\vec{k}}(\vec{r}) \ . \tag{11}$$

The G_i's are the reciprocal-lattice vectors of the bcc lattice,[6]

$$\vec{G}_i = (2\pi/a)[(h+l)\hat{x} + (h+k)\hat{y} + (k+l)\hat{z}] \ . \tag{12}$$

a is the lattice constant and h, k, l are integers. N is the number of atoms (cells) of the lattice. The integration is over a Wigner-Seitz polyhedron of volume

TABLE I. Experimental and theoretical Compton profile of Li. The normalization is $\int_0^{3 \text{ a.u.}} J(q)\, dq = 1$.

q (a.u.)	Present expt	One-electron theory Callaway	Seitz	RFA	Correlations (Lam)	RFA + Correlations
0.0	2.016 ± 2%	2.396	2.174	2.415	2.248	2.091
0.1	2.007	2.325	2.110	2.343	2.187	2.037
0.2	1.791	2.112	1.921	2.127	2.006	1.872
0.3	1.477	1.756	1.605	1.768	1.705	1.599
0.4	1.232	1.259	1.162	1.266	1.287	1.218
0.5	0.868	0.619	0.592	0.619	0.757	0.737
0.6	0.570	0.059	0.094	0.053	0.225	0.203
0.7	0.311	0.059	0.094	0.053	0.141	0.140
0.8	0.167	0.059	0.094	0.053	0.090	0.125
0.9	0.081	0.058	0.093	0.052	0.060	0.117
1.0	0.079	0.056	0.092	0.050	0.040	0.107
1.2	0.032	0.048	0.089	0.044	0.019	0.087
1.4	0.040	0.040	0.085	0.036	0.010	0.069
1.6	0.030	0.029	0.076	0.028	0.004	0.052
1.8	0.036	0.022	0.062	0.020	0.002	0.039
2.0	0.040 ± 6%	0.018	0.048	0.016	0.001	0.029
2.2	0.019	0.015	0.034	0.011	0.001	0.022
2.4	0.010	0.011	0.024	0.008	0.0	0.016
2.6	0.022	0.008	0.020	0.006		0.012
2.8	0.013	0.005	0.018	0.004		0.009
3.0	0.008 ± 15%	0.004	0.016	0.004		0.007

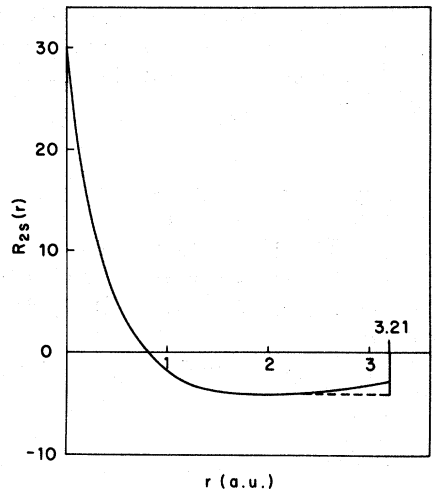

FIG. 5. 2s wave function for Li in the renormalized free-atom model. The dashed line indicates a simple way of satisfying the Wigner-Seitz condition at $r_s = 3.21$ a.u.

$$\Omega_0 = \tfrac{4}{3}\pi r_s^3 . \tag{13}$$

In the case where the above wave function (9) is employed, we have

$$\varphi_{\vec{k}}^c(\vec{p}) = \varphi_0^c(\vec{G}_i) , \tag{14}$$

$$\varphi_{\vec{k}}(\vec{p}) = N\delta_{\vec{p},\vec{k}+\vec{G}_i}\varphi_0^c(\vec{G}_i) . \tag{15}$$

In order to preserve the normalization of $\varphi_{\vec{k}}(\vec{p})$ while performing the integration in Eq. (11) over the Wigner-Seitz sphere, we rewrite the integral as follows:[11,20]

$$\varphi_{\vec{k}}^c(\vec{p}) = (2\pi)^{-3/2}\int_{\Omega_0} d\vec{r}\, e^{-i\vec{G}_i\cdot\vec{r}} \times[\varphi_0(\vec{r}) - \varphi_0(r_s)] + (2\pi)^{-3/2}\Omega_0\delta_{\vec{G}_i,0}\varphi_0(r_s). \tag{16}$$

The momentum density per atom is now

$$\rho(\vec{p}) = 2\sum_{\vec{k}}\delta_{\vec{p},\vec{k}+\vec{G}_i}|\varphi_0^c(\vec{G}_i)|^2 . \tag{17}$$

The summation is over the Bloch states and the factor 2 arises from the summation over spin. The wave functions used here are s-like wave functions. Thus the spherical average of $\rho(\vec{p})$ may be obtained by the method described by Berggren.[11] It is

$$\langle\rho(\vec{p})\rangle = 2\sum_{i=0}^{\infty} N_{G_i} n_i(p)|\varphi_0^c(G_i)|^2 . \tag{18}$$

N_{G_i} is the number of reciprocal-lattice vectors with length G_i and the coefficients $n_i(p)$ are, for $i \neq 0$,

$$n_i(p) = [p_F^2 - (G_i - p)^2]/4pG_i \quad \text{if } G_i - p_F \leq p \leq G_i + p_F$$

and

$$n_i(p) = 0 \quad \text{if } p > G_i + p_F \text{ or } p < G_i - p_F ; \tag{19}$$

while for $i = 0$,

$$n_0(p) = 1 \quad \text{if } p \leq p_F$$

and

$$n_0(p) = 0 \quad \text{if } p > p_F . \tag{20}$$

p_F is the Fermi momentum.

The Compton profile is then calculated from Eq. (6) to be

$$J(q) = 2\sum_{i=0}^{\infty}|\varphi_0^c(G_i)|^2 F_i(q) , \tag{21}$$

where

$$F_i(q) = N_{G_i}\int_q^{\infty} pn_i(p)\,dp . \tag{22}$$

The term for $i = 0$ in the expansion of $J(q)$ in Eq. (21) gives us (apart from a normalization factor) the free-electron parabola, that is, the Compton profile for a uniform (noninteracting) electron gas.[21] The higher terms give rise to a tail in the profile at $q > p_F$ which reflects the contribution of the lattice structure as described by the behavior of $\varphi_{\vec{k}}(\vec{r})$ in the cell.

Two sorts of wave-function calculations may be used in order to obtain the factors $|\varphi_0^c(\vec{G}_i)|^2$ in Eq. (21) according to the assumption in Eq. (10). We may either take lowest-order ($\vec{k} = 0$) wave functions obtained from a complete band-structure calculation assuming a self-consistent central potential[6,22] or, alternatively, we may compute wave functions in the renormalized free-atom model.[11]

B. Renormalized free-atom model

As discussed in Sec. III(A), one way of computing one-electron wave functions for lithium is by using the renormalized free-atom model which was employed by Berggren[11] for the interpretation of Compton-profile measurements in vanadium. The considerations that allow us to introduce this model in our case are the following: Assume that the core states are practically unchanged when introducing the (free) atom into a solid.[18] Then the wave function for a conduction electron in a state $\vec{k} = 0$ and the corresponding free-atom wave function are very much alike near the ion. The basis of our calculation is to take wave functions computed for a free atom,[16] to truncate them at $r = r_s$, and renormalize them within the Wigner-Seitz sphere (in order to preserve charge neutrality in it). We show in Fig. 5 the 2s wave function for lithium computed in this model. This funct

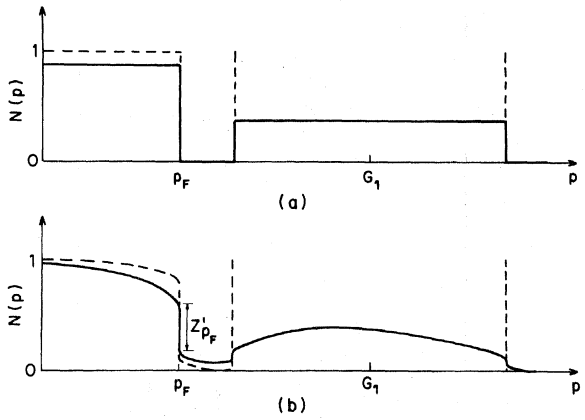

FIG. 6. Momentum density of an electron gas: (a) inhomogeneous, noninteracting; (b) (- - -) homogeneous interacting; (—) inhomogeneous interacting.

does not satisfy the boundary condition of Eq. (8) at r_s. The dashed line in the figure indicates a simple way due to Berggren[11] of satisfying Eq. (8), namely, beyond its minimum at r_{min} the function is set equal to a constant $R_{2s}(r_{min})$ and properly normalized. Berggren noticed that in the case of vanadium, this improvement did not lead to significant changes in the shape of the profile. In our case, the changes were found to be negligible only at $q=0$ (0.3%), but they were appreciable at $q>p_F$ (20% at $q=1$ a.u. and even 50% at $q=2$ a.u.).

C. Many-electron calculation

It is well known that Compton-profile measurements are sensitive to electron-electron correlations. Consider the many-body problem of an interacting electron gas submerged in an ordered lattice of ions. Assume here that the electron-ion interactions are well described by the one-electron model discussed above. The electronic system that is solved in the picture may be considered as unperturbed, while the electron-electron correlations are introduced as a perturbation. This is the basis of an approach due to Lundqvist and Lyden[9] and we shall use it here with some simplifying assumptions.

For clarification, we give in Fig. 6(a) a schematic description of $\rho(\vec{p})$ in the one-electron model. In this model the Fermi surface may be represented as an ensemble of spheres of equal radius p_F centered on each one of the reciprocal-lattice points,[21] and $\rho(\vec{p})$ is the corresponding momentum density. According to the geometry of the lattice, the different surfaces which appear may be completely separated from each other or partially overlapping. For a bcc lattice we always have $|\vec{G}_i| > 2p_F$ and therefore, at least the first surface (centered at $p=0$) must appear isolated from the other ones. To be more precise, each one of the surfaces is expected to be anisotropic in momentum space[5] but in the case of simple alkali metals, and in our experimental conditions (polycrystalline sample), the influence of this anisotropy on the profile is negligible. (From previous measurements,[3,9] the shift in the place of the Fermi momentum for different orientations of a single crystal of lithium is much less than our experimental uncertainty in momentum space.)

If electron-electron correlations are introduced now, the discontinuity in $\rho(\vec{p})$ at p_F is known to be reduced[23] and a tail appears at $p>p_F$ in the first surface. We expect to observe similar phenomena for the other surfaces centered at points $\vec{G}_i \neq 0$.[5] This is clarified in Fig. 6(b). The dashed line is the momentum density for a homogeneous interacting electron gas. The solid line is the result of a more complete calculation in the case of the so-called inhomogeneous interacting electron gas.[5] It has been shown[23,24] that the integral of $\rho(\vec{p})$ over the whole momentum space is conserved.

The momentum density expressed in terms of electron-field operators $\hat{\psi}(\vec{r},t)$ is[9]

$$\rho(\vec{p})=\frac{1}{\Omega}\int d\vec{r}_1\int_\Omega d\vec{r}_2\, e^{i\vec{p}\cdot(\vec{r}_1-\vec{r}_2)} \times\langle\hat{\psi}^\dagger(\vec{r}_1,0)\hat{\psi}(\vec{r}_2,0)\rangle\ , \tag{23}$$

where Ω is the volume of the crystal. It is always possible to expand the field operators in Bloch waves $\varphi_{\vec{k}}(\vec{r})$,

$$\hat{\psi}(\vec{r},0)=\sum_{\vec{k}} a^B_{\vec{k}}(0)\varphi_{\vec{k}}(\vec{r})\ , \tag{24}$$

where $a^B_{\vec{k}}(t)$ is the annihilation operator for an electron in a Bloch state. $\varphi_{\vec{k}}(\vec{r})$ may be expanded in plane waves,

$$\varphi_{\vec{k}}(\vec{r})=\sum_{\vec{G}_i}\varphi_{\vec{k}}(\vec{p})\,e^{i(\vec{k}+\vec{G}_i)\cdot\vec{r}}\ . \tag{25}$$

Using the coefficients $\varphi^c_{\vec{k}}(\vec{p})$ defined in Eq. (10), one obtains

$$\rho(\vec{p})=\frac{N}{\Omega}\int_{\Omega_0} d\vec{r}_1\int_{\Omega_0} d\vec{r}_2\, e^{i\vec{p}\cdot(\vec{r}_1-\vec{r}_2)}\left\langle\sum_{\vec{k},\vec{G}_i} a^{B\dagger}_{\vec{k}}(0)\varphi^{c*}_{\vec{k}}(\vec{p})\,e^{-i(\vec{k}+\vec{G}_i)\cdot\vec{r}_1}\delta_{\vec{k}+\vec{G}_i,\vec{p}}\sum_{\vec{k}'\vec{G}_j} a^B_{\vec{k}'}(0)\varphi^c_{\vec{k}'}(\vec{p})\,e^{i(\vec{k}'+\vec{G}_j)\cdot\vec{r}_2}\delta_{\vec{k}'+\vec{G}_j,\vec{p}}\right\rangle, \tag{26}$$

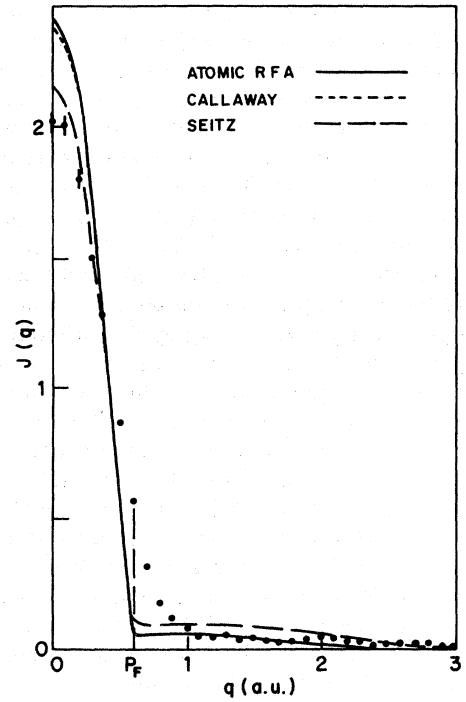

FIG. 7. Compton profile for lithium computed in the cell approximation and compared with experiment. Except in the small-momentum region, the profile computed with the help of Callaway functions coincides with that based on the renormalized free-atom model.

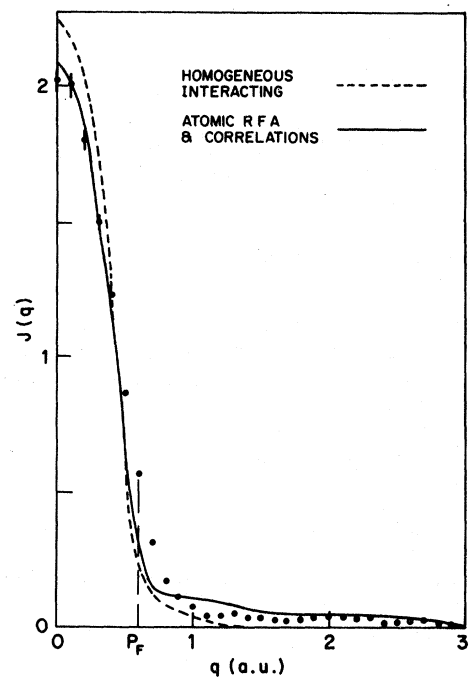

FIG. 8. Compton profile for lithium computed in the Lam method (correlations + exchange, Ref. 8) for homogeneous and inhomogeneous interacting electron gas, and compared with the experiment.

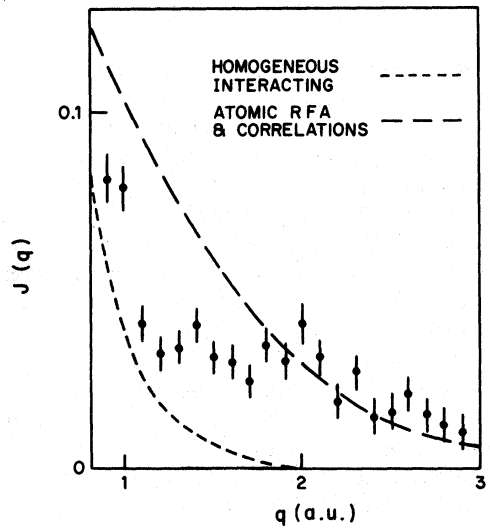

FIG. 9. High-momentum part of the Compton profile for lithium computed in the Lam method (correlations + exchange, Ref. 8) for homogeneous and inhomogeneous interacting electron gas, and compared with experiment.

or

$$\rho(\vec{p}) = \sum_{\vec{G}_i,\vec{G}_j} \varphi^*_{\vec{p}-\vec{G}_i}(\vec{p})\varphi_{\vec{p}-\vec{G}_j}(\vec{p}) \times \langle a^{B\dagger}_{\vec{p}-\vec{G}_i}(0)\, a^{B}_{\vec{p}-\vec{G}_j}(0)\rangle \ . \tag{27}$$

Following Lundqvist and Lyden,[9] we shall employ two assumptions:

(i) The terms with $\vec{k}=\vec{p}-\vec{G}_i \neq \vec{k}'=\vec{p}-\vec{G}_j$ give negligible contributions to the momentum density. Therefore,

$$\rho(\vec{p}) = \sum_{\vec{G}_i} |\varphi^c_{\vec{p}-\vec{G}_i}(\vec{p})|^2 n^B(\vec{p}-\vec{G}_i) \ , \tag{28}$$

where the n^B are the mean occupation numbers for Bloch states.

(ii) When the potential of the ions is weak, it is possible to introduce the electron-electron interactions by approximating the Bloch occupation numbers by the mean occupation numbers $n(k)$ calculated for an homogeneous interacting electron gas.

If we use instead of $|\varphi^c_{\vec{k}}(\vec{p})|^2$ the RFA terms $|\varphi^c_{\vec{k}}(\vec{G}_i)|^2$ of Eq. (17) the integration over angles is easily performed:

$$\langle \rho(\vec{p})\rangle = |\varphi^c_0(\vec{G}_i=0)|^2 n(p) + \frac{1}{2}\sum_{\vec{G}_i\neq 0} \frac{|\varphi^c_0(\vec{G}_i)|^2}{p|\vec{G}_i|} \int_{|\vec{p}-\vec{G}_i|}^{|\vec{p}+\vec{G}_i|} n(\xi)\,\xi\, d\xi \ . \tag{29}$$

$J(q)$ is thus obtained from Eq. (6).

IV. RESULTS AND DISCUSSION

For comparison with the experimental results we computed the theoretical profile for polycrystalline lithium in each of the models that was described above. In the present calculations we used the value $r_s = 3.21$ a.u. for lithium at metallic density.[6,22] This corresponds to a Fermi momentum $p_F = 0.599$ a.u. We show in Fig. 7 and in Table I the profiles computed in the cell approximation using Eq. (21). The wave functions employed here were of two forms:

(a) The RFA wave function shown in Fig. 5.

(b) Callaway[22] and Seitz[6] wave functions computed in the cell approximation (at the lowest order in $\vec{k}$). The coefficients $|\varphi_0^c(\vec{G}_i)|^2$ that were obtained in our calculation for the Seitz function differed slightly from the results of Donovan and March.[6] However, the normalization condition $\sum a_i |\varphi_0^c(\vec{G}_i)|^2 = 1$ was satisfied and it is probable that the difference is mainly due to our integration procedure in Eq. (16). It is seen that all the profiles computed in this model have a value at $q = 0$ which is much larger than the experimental value, have a break at $q = p_F$ and a large tail beyond it.

The profile for an homogeneous interacting electron gas with the same electronic density as lithium was computed in a method due to Lam[8] which takes into account the Coulomb correlations and some exchange properties between the electrons. (The latter reduce the probability of short-range interactions and decrease the size of the tail at $p > p_F$, but this change is not very significant.) This curve is presented in Fig. 8 and in Table I with the experimental results. Compared with the one-electron calculations, there is no improvement here at $q = 0$ but it must be noticed that the curve goes to zero at $q \sim 2$ a.u. Thus one cannot expect the contribution of electrons at higher momenta to arise from electron-electron interactions. The curve $J(q)$ based on Eq. (29) is also presented in Fig. 8 and in Table I. Here the $|\varphi_0^c(\vec{G}_i)|^2$ coefficients are the RFA ones and the $n(k)$ numbers are those computed in the Lam method.[8] The results are not appreciably different when the $|\varphi_0^c(\vec{G}_i)|^2$ coefficients are computed with Seitz or Callaway wave functions. It is seen that the value of the calculated profile at $q = 0$ is now in good agreement with the experimental result. In Fig. 9 we show in more detail the high-momentum part of Fig. 8. At $q > 2$ a.u. the agreement between the experimental points and our inhomogeneous-interacting-electron-gas calculation is quite good. Thus one may attribute the existence in the profile of the large high momentum tail to dominating electron-ion interaction. This is in agreement with the study of Eisenberger *et al.*[5] for $q \leq 1.6$ a.u. It is interesting to note that our results contradict the conclusion of Phillips and Weiss, who attributed the existence of the tail in the profile mainly to electron-electron correlations.

---

*This research is a part of a thesis submitted by S. W. in partial fulfillment for the M. Sc. degree.

†This author's name has recently been changed from Raymond Fox to Reuven Opher.

[1] M. Cooper, B. G. Williams, R. E. Borland, and J. R. A. Cooper, Philos. Mag. 22, 441 (1970).

[2] R. E. Borland and J. R. A. Cooper, J. Phys. C 3, 5253 (1970).

[3] W. C. Phillips and R. J. Weiss, Phys. Rev. 171, 790 (1968).

[4] W. C. Phillips and R. J. Weiss, Phys. Rev. B 5, 755 (1972).

[5] P. Eisenberger, L. Lam, P. M. Platzman, and P. Schmidt, Phys. Rev. B 6, 3671 (1972).

[6] B. Donovan and N. H. March, Proc. Phys. Soc. Lond. 69, 1249 (1956).

[7] E. Daniel and S. H. Vosko, Phys. Rev. 120, 2041 (1960).

[8] J. Lam, Phys. Rev. B 3, 3243 (1971).

[9] B. J. Lundqvist and C. Lyden, Phys. Rev. B 4, 3360 (1971).

[10] B. W. Tan, J. Phys. F 3, 1716 (1973).

[11] K. F. Berggren, Phys. Rev. B 6, 2156 (1972).

[12] J. Felsteiner, R. Fox, and S. Kahane, Phys. Rev. B 6, 4689 (1972).

[13] J. Felsteiner, P. Pattison, and M. Cooper, Philos. Mag. 30, 537 (1974); J. Felsteiner and P. Pattison, Nucl. Instr. Meth. (to be published).

[14] P. Eisenberger and W. A. Reed, Phys. Rev. A 5, 2085 (1972).

[15] K. H. Lloyd, Am. J. Phys. 37, 329 (1969).

[16] R. Currat, P. D. deCicco, and R. J. Weiss, Phys. Rev. B 4, 4256 (1971).

[17] F. Herman and S. Skillman, *Atomic Structure Calculations* (Prentice Hall, Englewood Cliffs, N. J., 1963).

[18] See, e.g., J. M. Ziman, *Principles of the Theory of Solids* (Cambridge U. P., Cambridge, 1971).

[19] J. Bardeen, J. Chem. Phys. 6, 367 (1938).

[20] S. Berko and J. S. Plaskett, Phys. Rev. 112, 1877 (1958).

[21] M. Cooper, Adv. Phys. 20, 453 (1971).

[22] J. Callaway and W. Kohn, Phys. Rev. 127, 1913 (1962).

[23] A. B. Migdal, Zh. Eksp. Teor. Fiz. 32, 399 (1957). [Sov. Phys.–JETP 5, 333 (1957)].

[24] J. M. Luttinger, Phys. Rev. 119, 1153 (1960).